Direct Observation of a Transition of a Surface Plasmon Resonance from a Photonic Crystal Effect

Weili Zhang, Abul K. Azad, and Jiaguang Han
School of Electrical and Computer Engineering, Oklahoma State University, Stillwater, Oklahoma 74078, USA

Jingzhou Xu, Jian Chen, and X.-C. Zhang
Center for THz Research, Rensselaer Polytechnic Institute, Troy, New York 12180, USA
(Received 24 March 2006; published 1 May 2007)

Transition of surface-plasmon resonance from out-of-plane photonic crystal effect is observed in a semiconductor array of subwavelength holes by optical pump-terahertz probe measurements. The dielectric properties of the photoexcited array are essentially altered by the intense optical excitation due to photogenerated free carriers. As a result, the array becomes metallic and favors the coupling and propagation of surface plasmons. The photoinduced resonant extremes agree well with the Fano model.

DOI: 10.1103/PhysRevLett.98.183901 PACS numbers: 42.70.Qs, 42.65.Re, 73.20.Mf

Manipulation of electromagnetic waves below wavelength scale is vital in broad disciplinary applications of photonics and has been a challenging task for decades. Recent demonstration of extraordinary transmission of light through an array of metallic nanostructures has opened up a new avenue to subwavelength photonics [1,2]. This fascinating phenomenon, understood as resonant excitation of surface plasmons (SPs) at the metal-dielectric interface, has been extensively explored in a wide spectral range, and is very promising in nanolithography, near-field microscopy, integrated photonic devices, and biochemical sensing [3–16].

At terahertz frequencies, in addition to metals, semiconductors with high density of free carriers show metallic properties by having a negative real part of dielectric function ($\varepsilon_{r2} < 0$), and thus can be used as alternate metallic media to support SPs [14,15]. The advantage of semiconductors is that their dielectric function can be modified by varying doping concentration, temperature, or optical excitation. This in turn enables tuning and switching of SPs. Recently, SP-enhanced terahertz transmission in highly doped semiconductor gratings was observed [14,15] and was effectively tuned to a reduced transmission level by optical switching [17]. However, it is intriguing how SP resonance can be evolutionally developed when the real part of dielectric function of the constituent medium is altered instantaneously from positive, across zero, to negative.

In this Letter, we present observation of a characteristic evolution of SP resonance in a semiconductor subwavelength hole array by use of optical pump-terahertz probe measurements. The array was made from lightly doped silicon (Si), which does not support SPs due to low carrier density, but exhibits out-of-plane two-dimensional (2D) photonic crystal effect [18]. When optical excitation is applied to the array, the photogenerated free carriers alter the dielectric properties of Si; the real part of the dielectric constant changes from positive to negative with increasing excitation intensity. As a result, the signature of photonic crystal effect gradually disappears and SP resonance emerges and is developed into extraordinary terahertz transmission. The resonance profiles of the SP modes are well described by the Fano model.

The array sample was fabricated from commercially available 30 μm thick n-type Si with 10Ω cm resistivity and 4×10^{14} cm^{-3} carrier concentration. The periodic through holes were processed by standard microfabrication as described previously [15]. The sample is a 10 mm $\times$ 10 mm-sized array of 80 μm $\times$ 40 μm elliptical holes in a square lattice with a periodicity of 160 μm, as shown in the inset of Fig. 1. Conventional optical pump-terahertz probe [19] characterization is carried out by use of an electro-optic terahertz system [20]. The terahertz beam is collimated to a diameter of $\sim$1.50 mm on the array, while the beam of optical excitation (100 fs, 1 kHz) has a greater size and overlaps well with the terahertz spot.

Terahertz transmission measurements were performed at a normal incidence with p-polarized terahertz field. Figure 1(a) illustrates the transmitted terahertz pulses through air reference, blank Si, and the array of both perpendicular and parallel orientations before and after the optical excitation of a 111 mW average power. The perpendicular (parallel) orientation of the array is defined with the longer axis of the elliptical hole perpendicular (parallel) to the terahertz electric field. The transmitted terahertz pulse through the unexcited blank Si shows $\sim$85% field transmission if surface reflections are taken into account; then the Si becomes nearly opaque to terahertz waves under intense optical excitation due to strong absorption of photogenerated free carriers. The corresponding Fourier-transformed spectra are shown in Fig. 1(b). In the absence of optical excitation the array can be considered as a two-dimensional out-of-plane photonic crystal slab that has shown complicated spectral

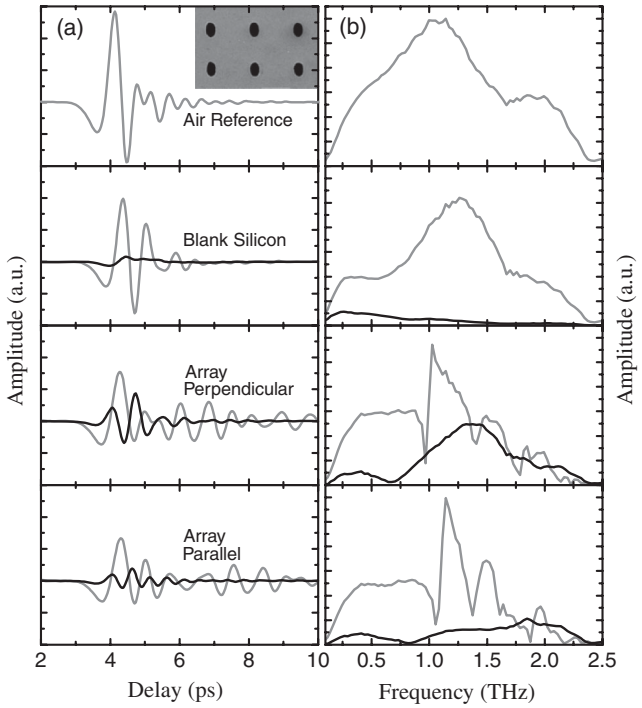

FIG. 1. (a) Measured transmitted terahertz pulses and (b) the corresponding Fourier-transformed spectra through air reference, blank Si, Si array of perpendicular, and parallel orientations with (black curves) and without (gray curves) optical excitation at an 111 mW average power. The inset shows the scanning electron microscopic image of the Si array of elliptical through holes.

structures instead of stop gaps [18]. Under intense optical excitation, however, the transmission spectra exhibit totally different features; the photonic crystal resonances disappear and SP resonance peaks occur at different frequencies.

The SP resonance modes are approximately described by the dispersion relation for 2D metallic gratings at normal incidence [21,22]

$$\lambda_{\mathrm{SP}}^{m,n} = \frac{L}{\sqrt{m^2+n^2}}\,\mathrm{Re}\left(\sqrt{\frac{\varepsilon_1\varepsilon_2}{\varepsilon_1+\varepsilon_2}}\right), \qquad (1)$$

where L is the lattice constant, m and n are the integer mode indices, and ε_1 is the dielectric constant of surrounding medium; here $\varepsilon_1 = 1$ for air, and $\varepsilon_2 = \varepsilon_{r2} + i\varepsilon_{i2}$ is the complex dielectric constant of metallic medium. The metallic behavior of the array is mainly determined by the negative value of the real dielectric constant $\varepsilon_{r2} < 0$. Under intense optical excitation, the Si array becomes a complex multilayer medium, composed of a stack of photoexcited Si and unexcited Si layers. At terahertz frequencies, ε_{r2} of the photoexcited layer may turn to negative from being positive under appropriate laser excitation and hence the sample behaves as a metallic array that favors the formation of SPs. The thickness of the photoexcited layer depends on the penetration depth δ_L at the excitation laser wavelength; here $\delta_L = 10\ \mu$m for Si at $\lambda = 800$ nm [23]. In contrast, the penetration depth (or skin depth) for terahertz waves in the photoexcited Si is $\delta_{\mathrm{THz}} = 3.69\ \mu$m at 1.50 THz under 111 mW excitation [21], corresponding to a carrier density $N = 0.99 \times 10^{18}$ cm^{-3}. δ_{THz} is influenced by laser intensity; it becomes thinner with increasing optical excitation.

The frequency-dependent terahertz transmission of the array under 111 mW optical excitation for both orientations is plotted in Fig. 2. Transmission enhancement is observed at the fundamental SP 1.50 $[\pm 1, 0]$ THz mode for perpendicular orientation, and 1.85 $[0, \pm 1]$ THz for parallel orientation occurred at the metallic Si-air interface [15]. The orientation-dependent transmission property is consistent with previous work reported in both visible and terahertz regions [15,24]. In addition, a transmission minimum occurs in the spectra at 1.95 THz due to Wood's anomaly [8,15,25].

The resonant terahertz transmission through the photoinduced metallic Si array is analyzed by the typical Fano model, which involves two types of scattering processes, the continuous direct scattering state and the discrete resonant state [26],

$$T(\omega) = T_a + T_b\left(1 + \sum_v \frac{q_v}{\varepsilon_v}\right)^2 \Big/ \left[1 + \left(\sum_v \frac{1}{\varepsilon_v}\right)^2\right], \qquad (2)$$

where $\varepsilon_v = (\omega - \omega_v)/(\Gamma_v/2)$, T_a is associated with the direct penetration, and $|T_b|$ is the contribution from a zero-order continuum state that couples with the discrete reso-

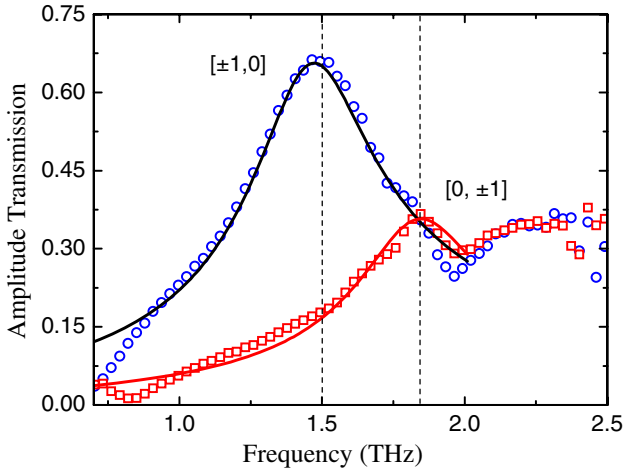

FIG. 2 (color online). Measured (dots) and the Fano profiles (solid curves) of frequency-dependent terahertz transmission through the Si array in both perpendicular and parallel orientations under 111 mW optical excitation. The vertical dashed lines represent the resonance peaks. The fitting parameters are $q_v = 12.59 \pm 0.2$, $\omega_v/2\pi = 1.46 \pm 0.05$ THz, $\Gamma_v/2\pi = 0.43 \pm 0.05$ THz, and $T_b = (2.7 \pm 0.1) \times 10^{-3}$ for the $[\pm 1, 0]$ mode; and $q_v = 12.59 \pm 0.2$, $\omega_v/2\pi = 1.81 \pm 0.05$ THz, $\Gamma_v/2\pi = 0.45 \pm 0.05$ THz, and $T_b = (0.8 \pm 0.1) \times 10^{-3}$ for the $[0, \pm 1]$ mode.

nant state. The resonant state is characterized by resonant frequency ω_v, linewidth Γ_v, and the Breit-Wigner-Fano coupling coefficient q_v [27–30]. As shown in Fig. 2, the Fano profiles agree well with the measured fundamental resonances at 111 mW optical excitation [28,29].

To explore the characteristic evolution of the photoinduced SP resonance, the laser excitation was varied from 0 to 111 mW. Figure 3 shows the dependence of the complex dielectric constant of the photoexcited Si layer at 1.50 THz, the $[\pm 1, 0]$ SP mode, on laser excitation power. The dielectric constant was measured from the reference Si slab where the power absorption α and the refractive index n of the photoexcited Si layer were determined by comparing the transmitted terahertz pulses through the photoexcited and unexcited slab. The dielectric constant was obtained from α and n using the relations $\varepsilon_{r2} = n^2 - k^2$ and $\varepsilon_{i2} = 2nk$, where $k = \alpha c/(2\omega)$ [31].

As expected, the real dielectric constant ε_{r2} is evolutionally tuned from positive, across zero, to negative with increasing optical power. Above 3 mW, the photoexcited Si layer begins to exhibit metallic properties and has potential to support SPs. Figure 4 illustrates frequency-dependent terahertz transmission through the array of perpendicular orientation under various optical intensities. At low excitation, the transmission is dominated by complex out-of-plane photonic crystal resonances near 0.97, 1.40, and 1.78 THz. When the laser power is increased to 12.5 mW, the photonic crystal effect nearly disappears; a new resonance peak occurs at 1.60 THz due to the excitation of SPs. The further increase in excitation power gives rise to an enhanced terahertz transmission and a redshift of resonance peak to 1.50 THz.

The transmission efficiency at the SP resonance 1.50 THz is found to increase with increasing power of laser excitation. At 25 mW, the maximum terahertz transmittance is 25.5%, while it is increased to 45% at 111 mW, corresponding to a 340% transmittance when normalized to the area of the holes. From the pump-dependent dielectric function shown in Fig. 3, the phenomenon can be understood that the photoexcited Si layer shows improved metallic properties with increasing optical excitation and hence favors the establishment of SPs [32].

It is worth noting that, when optical excitation is increased above 12.5 mW, narrowing of resonance linewidth occurs as shown in Fig. 5, indicating that the damping of SPs becomes less intense. Generally, the total damping of SPs is described by $\Gamma = \Gamma_1 + \Gamma_2$, where Γ_1 is internal damping due to loss at metallic surface and Γ_2 is radiative damping associated mainly with hole size [21,33]. At various optical excitations, the effective size of holes is skin-depth dependent, $d_{\text{eff}} = d_0 + 2\delta_{\text{THz}}$, with d_0 the nominal hole width [17]. In our case, the effective hole width is reduced from 48.7 to 47.4 μm with increasing excitations from 25 to 111 mW. Such a slight variation in hole width will not cause obvious change in Γ_2 [33]. This is also confirmed by the resonance frequency that exhibits no shift under excitations above 25 mW [17,33]. Therefore, the excitation dependent linewidth reduction is mainly originated from the change in Γ_1; the improved metallic

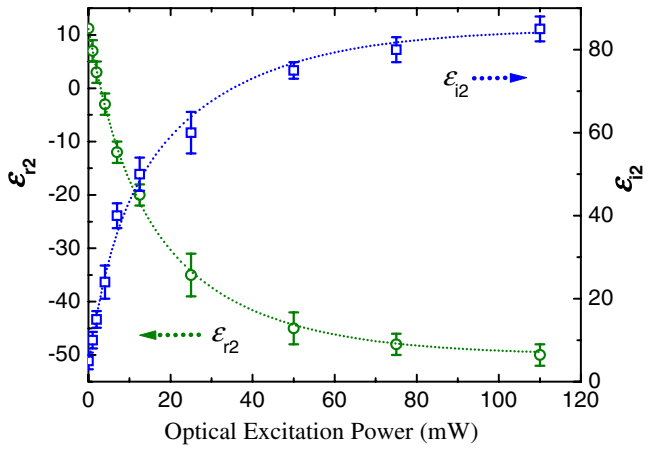

FIG. 3 (color online). Measured dielectric constant of photoexcited Si at 1.50 THz as a function of optical excitation. The real (ε_{r2}) and imaginary (ε_{i2}) dielectric constants are represented by open circles and squares, respectively. The dotted curves are to guide the eye.

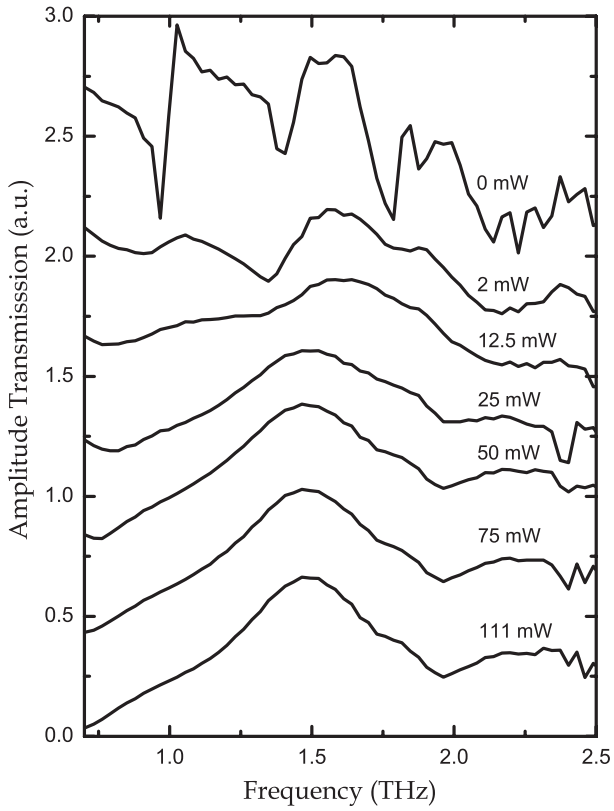

FIG. 4. Frequency-dependent terahertz transmission through the array of perpendicular orientation under various laser excitations ranging from 0 to 111 mW. The measurements for different optical excitations are vertically shifted for clarity.

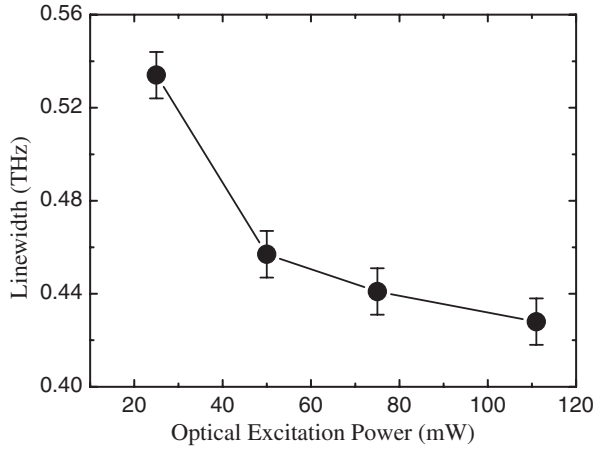

FIG. 5. Measured resonance linewidth of the SP $[\pm 1, 0]$ mode as a function of optical excitation power. The dotted curve is to guide the eye.

properties with increasing optical excitation enable SPs to be well pronounced [32].

In summary, we present a characteristic transition of SP resonance from the out-of-plane photonic crystal resonances observed in a semiconductor subwavelength hole array by optical pump-terahertz probe measurements. The photogenerated free carriers have tuned the permittivity of the dielectric array so that it becomes metallic, thus enables the establishment of SPs at the Si-air interface. The measured transmittance of the fundamental SP modes is found to be enhanced with increasing optical excitation due to improved metallic properties. These findings demonstrate a new path to tunable SPs; particularly, the ultrafast tuning of SPs will be feasible in arrays made from semiconductors with fast carrier lifetime.

The authors acknowledge Yuguang Zhao for help with the sample fabrication. This work was partially supported by the National Science Foundation and the Oklahoma EPSCoR for the National Science Foundation. A. K. A. is now with the Los Alamos National Laboratory. The Rensselaer team was supported by the National Science Foundation and the Army Research Office.

[1] T. W. Ebbesen, H. J. Lezec, H. F. Ghaemi, T. Thio, and P. A. Wolff, Nature (London) **391**, 667 (1998).
[2] W. L. Barnes, A. Dereux, and T. W. Ebbesen, Nature (London) **424**, 824 (2003).
[3] R. Gordon, A. G. Brolo, A. McKinnon, A. Rajora, B. Leathem, and K. L. Kavanagh, Phys. Rev. Lett. **92**, 037401 (2004).
[4] K. J. Klein Koerkamp, S. Enoch, F. B. Segerink, N. F. van Hulst, and L. Kuipers, Phys. Rev. Lett. **92**, 183901 (2004).
[5] W.-C. Tan, T. W. Preist, and R. J. Sambles, Phys. Rev. B **62**, 11 134 (2000).
[6] D. Qu, D. Grischkowsky, and W. Zhang, Opt. Lett. **29**, 896 (2004).
[7] F. Miyamaru and M. Hangyo, Appl. Phys. Lett. **84**, 2742 (2004).
[8] G. Torosyan, C. Rau, B. Pradarutti, and R. Beigang, Appl. Phys. Lett. **85**, 3372 (2004).
[9] J. O'Hara, R. D. Averitt, and A. J. Taylor, Opt. Express **12**, 6397 (2004).
[10] H. Cao and A. Nahata, Opt. Express **12**, 1004 (2004).
[11] D. Qu and D. Grischkowsky, Phys. Rev. Lett. **93**, 196804 (2004).
[12] A. K. Azad and W. Zhang, Opt. Lett. **30**, 2945 (2005).
[13] B. Pradarutti, C. Rau, G. Torosyan, and R. Beigang, Appl. Phys. Lett. **87**, 204105 (2005).
[14] J. Gómez Rivas, C. Schotsch, P. Bolivar, and H. Kurz, Phys. Rev. B **68**, 201306(R) (2003).
[15] A. K. Azad, Y. Zhao, and W. Zhang, Appl. Phys. Lett. **86**, 141102 (2005).
[16] S. S. Akarca-Biyikli, I. Bulu, and E. Ozbay, Appl. Phys. Lett. **85**, 1098 (2004).
[17] C. Janke, J. G. Rivas, P. H. Bolivar, and H. Kurz, Opt. Lett. **30**, 2357 (2005).
[18] Z. Jian and D. Mittleman, Appl. Phys. Lett. **87**, 191113 (2005).
[19] B. I. Greene, John F. Federici, D. R. Dykaar, A. F. J. Levi, and L. Pfeiffer, Opt. Lett. **16**, 48 (1991).
[20] B. Ferguson and X.-C. Zhang, Nat. Mater. **1**, 26 (2002).
[21] H. Raether, *Surface Plasmons on Smooth and Rough Surfaces and on Gratings* (Springer-Verlag, Berlin, 1988).
[22] H. F. Ghaemi, T. Thio, D. E. Grupp, T. W. Ebbesen, and H. J. Lezec, Phys. Rev. B **58**, 6779 (1998).
[23] G. P. Agrawal, in *Fiber-Optic Communication Systems*, Wiley Series in Microwave and Optical Engineering (Wiley Interscience, New York, 2003).
[24] R. Gordon, M. Hughes, B. Leathem, K. L. Kavanagh, and A. G. Brolo, Nano Lett. **5**, 1243 (2005).
[25] R. W. Wood, Phys. Rev. **48**, 928 (1935).
[26] U. Fano, Phys. Rev. **124**, 1866 (1961).
[27] C. Genet, M. P. Van Exter, and J. P. Woerdman, Opt. Commun. **225**, 331 (2003).
[28] W. Fan, S. Zhang, B. Minhas, K. J. Malloy, and S. R. J. Brueck, Phys. Rev. Lett. **94**, 033902 (2005).
[29] J. B. Masson and G. Gallot, Phys. Rev. B **73**, 121401 (2006).
[30] S. H. Chang, S. K. Gray, and G. C. Schatz, Opt. Express **13**, 3150 (2005).
[31] M. C. Beard, G. M. Turner, and C. A. Schmuttenmear, Phys. Rev. B **62**, 15 764 (2000).
[32] T. Thio, H. F. Ghaemi, H. J. Lezec, P. A. Wolff, and T. W. Ebbesen, J. Opt. Soc. Am. B **16**, 1743 (1999).
[33] Jiaguang Han, Abul K. Azad, Mufei Gong, and Weili Zhang (unpublished).